

Correction to the heat-balance equation and its influence on velocity selection in dendritic growth

M.-A. Lemieux and G. Kotliar

Department of Physics, Massachusetts Institute of Technology, Cambridge, Massachusetts 02139

(Received 21 May 1987)

We propose a curvature correction to the heat-balance equation at the solid-melt interface that should be included in any realistic model of dendritic growth. Numerical evidences are presented to show that this term allows for steady-state solutions in the absence of anisotropy in the two-dimensional nonlocal symmetric model of solidification. It is shown that these solutions can be conjectured analytically in the large undercooling limit. Steady-state solutions are also obtained when anisotropy is added.

INTRODUCTION

It is now generally recognized that microscopic physical quantities can be of crucial importance in the velocity selection of steady-state solutions in dendritic growth via the microscopic solvability condition.¹⁻³ The microscopic solvability idea forces us to reconsider carefully the equations used to model dendritic growth since any new small term can have a drastic influence on the selection of the velocity. The first example of such an additional perturbation is surface tension. As is now well known,^{4,5} it is a singular perturbation that does not allow for any steady-state solution. The addition of anisotropy to the surface tension^{4,5} then yields a discrete family of steady-state solutions. Another example that was recently investigated is kinetic undercooling, and it was found⁶ that this term also acts as a singular perturbation. Anisotropy was again essential in order to get steady-state solutions.

In Sec. I of this paper we will propose and justify a correction that should be included in the heat-balance equation of any realistic model of solidification. This correction is very similar to the Gibbs-Thomson correction to the temperature of the interface.

In Sec. II we investigate the influence of this new term on the microscopic solvability condition. We present the results of numerical calculations done with the two-dimensional symmetric nonlocal model of solidification and include the effects of this new correction. It is found that the curvature correction to the latent heat allows for steady-state solutions in the absence of anisotropy. As will be shown these solutions are, however, not in a regime where the model is expected to be, strictly speaking, valid, because the capillary correction to the latent heat becomes of order unity. It is also possible to get anisotropy-induced solutions; we study in detail the velocity of these solutions as a function of the new curvature correction, of the anisotropy, and of the undercooling.

In the Appendix we look at the model in the large undercooling limit and in the absence of anisotropy and conjecture how these new anisotropy-free solutions would appear in an analytical treatment.

I. THERMODYNAMICS OF THE INTERFACE

In this section we will derive the correct boundary conditions at the solid-liquid interface for the temperature field. We will propose a new correction to the heat-balance equation very similar to the Gibbs-Thomson correction. The physical origin of this new term is a result of the conservation of energy. As the crystal grows, the area of the solid-melt interface increases. Energy is needed to create this new area, and therefore a part of the latent heat released in the solidification process is stored as interfacial energy in the additional interface. The local change in area being directly proportional to the local curvature, it should come as no surprise that a curvature-dependent correction is needed to conserve energy.

To derive the new boundary condition let us consider a *spherical solid of radius R* immersed in its melt, and assume that the interface is molecularly rough. Both the solid and the liquid are at temperature T . The pressure of the liquid P_L is fixed and equal to the pressure of the surrounding vessel. The pressure of the solid is⁷

$$P_S = P_L + \gamma\kappa, \quad (1)$$

where κ is the interface curvature, defined as positive when the radius lies in the solid. Equation (1) defines γ as the surface tension. The chemical potentials of both phases are related by^{7,8}

$$\mu_S(P_S, T) = \mu_L(P_L, T) + \kappa(\gamma - f)/\rho, \quad (2)$$

where ρ is the density of particles in the solid and f is the surface free energy per unit area. It is often assumed that γ and f are equal; this is true for a fluid-fluid interface but not correct in general for a solid-fluid interface, as was stressed by Gibbs and Cahn. The physical difference is related to the difference in the work done to *stretch* the surface, compared to the work done to *form* the surface.⁹

The equilibrium temperature is given by Eq. (2), and an approximate expression for T , as is well known, can be obtained by using the analyticity of the chemical potential. One first notes that for a planar interface

$P_S = P_L$ by Eq. (1) and then $\mu_S(P_L, T_M) = \mu_L(P_L, T_M)$ by Eq. (2), where T_M is by definition the melting temperature of the solid. One expands Eq. (2) in a Taylor series around the planar point (P_L, T_M) . For simplicity we will assume that the solid density is equal to the liquid density (since in Sec. II we will use a symmetric model of growth); it is, however, straightforward to write general expressions following the same line of thought. Using $P_S - P_L = \gamma\kappa$ and various Maxwell relations one finds

$$T = T_M(1 - d_0\kappa), \quad d_0 = f/L, \quad (3)$$

where $L = T_M(\eta_L(P_L, T_M) - \eta_S(P_L, T_M))$ is the latent heat per unit volume and $\eta_L(P_L, T_M) - \eta_S(P_L, T_M)$ is the difference in entropy per unit volume between the liquid and the solid. This is the Gibbs-Thomson condition.

We can now compute the amount of heat released in the liquid if the solid grows infinitesimally and changes its radius by an amount δR . Let S_1 be the solid's surface before the growth and S_2 be the surface afterwards. The change of energy inside S_2 is

$$\delta E = \int [\varepsilon_S(P_S, T) - \varepsilon_L(P_L, T)] \delta R dS + \int \varepsilon\kappa \delta R dS, \quad (4)$$

where $\varepsilon_S, \varepsilon_L$ are the internal energies per unit volume of the solid and the liquid and ε is the internal energy per unit area of the interface. Here dS is an infinitesimal element of surface, so that $\int \delta R dS$ is the change in volume and $\int \varepsilon\kappa \delta R dS$ is the change in area.

Using the definition of internal energy, we can write

$$\begin{aligned} & \varepsilon_S(P_S, T) - \varepsilon_L(P_L, T) \\ &= T(\eta_S(P_S, T) - \eta_L(P_L, T)) - (P_S - P_L) \\ & \quad + \rho(\mu_S(P_S, T) - \mu_L(P_L, T)). \end{aligned} \quad (5)$$

The last two terms are easy to evaluate given Eqs. (1) and (2). To evaluate $T(\eta_S(P_S, T) - \eta_L(P_L, T))$ we use Eq. (3) for T and expand the entropies in a Taylor series around the planar point (P_L, T_M) . Ignoring terms of order κ^2 , we find

$$\begin{aligned} & T(\eta_S(P_S, T) - \eta_L(P_L, T)) \\ &= -L + f\kappa + T_M\gamma\kappa(\partial\eta_S/\partial P)_{T,N} \\ & \quad + T_M^2 f\kappa[(\partial\eta_L/\partial T)_{P,N} \\ & \quad - (\partial\eta_S/\partial T)_{P,N}]/L, \end{aligned} \quad (6)$$

where the derivatives are evaluated at (P_L, T_M) . Thus

$$\delta E = - \int L \delta R dS + \int \{ \varepsilon + T_M\gamma(\partial\eta_S/\partial P)_{T,N} + T_M^2 f[(\partial\eta_L/\partial T)_{P,N} - (\partial\eta_S/\partial T)_{P,N}]/L \} \kappa \delta R dS. \quad (7)$$

Remembering the equal density assumption it is clear that there is no work done by the world *outside* S_2 during this transformation; hence, by the first law of thermodynamics we have $\delta E = \delta Q$. [If the densities were to be unequal then there would be some work done associated to the change of specific volume. This would simply add an extra term to Eq. (8) but would not change our conclusions.] If the transformation occurs during a time interval δt then

$$\delta E = \delta Q = - \int q_n \delta t dS, \quad (8)$$

where q_n is the flux of heat normal to the interface and is directed towards the liquid. Using $\delta R/\delta t = v_n$, the normal velocity of the interface, we finally find

$$c_S D_S \partial T/\partial n|_S - c_L D_L \partial T/\partial n|_L = q_n = L v_n (1 - d_1 \kappa), \quad (9a)$$

with

$$\begin{aligned} d_1 = L^{-1} \{ & \varepsilon + T_M\gamma(\partial\eta_S/\partial P)_{T,N} \\ & + T_M^2 f[(\partial\eta_L/\partial T)_{P,N} - (\partial\eta_S/\partial T)_{P,N}]/L \}. \end{aligned} \quad (9b)$$

Equations (9a) and (9b) are the important results of this section. Here c_S, c_L and D_S, D_L are the heat capacities per unit volume at constant pressure and the thermal diffusion constants. $\partial/\partial n$ is the gradient normal to the interface.

Using the thermal expansivity α and the isothermal compressibility k the previous expression may be rewritten as

$$\begin{aligned} d_1 = L^{-1} [& \varepsilon + T_M\gamma k \eta_S \\ & + T_M f(c_L - c_S)/L - T_M(\gamma + f)\alpha], \end{aligned} \quad (9c)$$

where the same values for α and k were used for both phases since we assumed equal densities. The derivation of Eqs. (9) assumed the solid to be spherical; the expressions obtained will, however, be valid for solids of general shape as long as we can assume local equilibrium.

Note finally that the new term d_1 is expected to increase the growth velocity and therefore has a destabilizing effect. The Mullins-Sekerka dispersion relation,¹⁰ describing the growth rate of a perturbation of wave vector k on a planar front according to $\delta\zeta_k(t) = \exp(\omega t)\delta\zeta_k(0)$, is indeed easily found to be, when $D_S = D_L$ and $c_S = c_L$,

$$\omega \approx vk(1 + d_1 k - 2d_0 D k^2/v) \quad (10)$$

in the limit $2kD/v \gg 1$ and $\omega \ll Dk^2$. The particular quadratic signature of the d_1 term should make its experimental detection possible by following the time development of instabilities on a planar front. The amplitudes of the Fourier components of the front's Fourier spectrum should behave according to Eq. (10), thereby making the detection of the quadratic term possible.

Since the d_1 term effectively diminishes the amount of heat that has to be released into the liquid [Eq. (9a)] we

can expect its presence to speed up the interface and favor the appearance of steady-state solutions.

II. NUMERICAL RESULTS

In this section we investigate how the new d_1 term affects the solvability condition and the selection of the steady-state velocity. We present the results of a study of the two-dimensional symmetric model of solidification of a pure substance when the d_1 term is included in the heat-balance equation.

A. The symmetric model

Let us now precisely state the nature of the model that we used. The model is called "symmetric" because $c_S = c_L = c$, $D_S = D_L = D$, and ρ is equal in both phases.¹¹

$$\Delta - d'_0 \kappa [\zeta(x)] = \pi^{-1} \int_{-\infty}^{\infty} dx' \{1 - d'_1 \kappa [\zeta(x')]\} \exp[\zeta(x') - \zeta(x)] K_0(\{(x - x')^2 + [\zeta(x) - \zeta(x')]^2\}^{1/2}), \quad (12)$$

where $\zeta(x, t) = \zeta(x) + vt$ is the position of the interface and is the sought steady-state solution, K_0 is a modified Bessel function, and

$$\Delta = (T_M - T_\infty)c/L = (\pi p)^{1/2} \exp(p) \operatorname{erfc}(p^{1/2}),$$

where p is the Péclet number. d'_0, d'_1 are the rescaled d_0, d_1 ,

$$d'_0 = T_M c f v / 2DL^2, \quad d'_1 = \varepsilon v / 2DL. \quad (13)$$

We will define the ratio $R \equiv d'_1 / d'_0$, which is v independent and is given for any substance, $R = \varepsilon L / f c T_M$. The parameters used numerically will be d'_0 and R . For a given R we will seek a selected value of d'_0 .

In principle, R can take any positive value. Indeed, $R = (\varepsilon/f)(L/T_M c)$ and the only thermodynamical constraint is that $\varepsilon > f$ since $\varepsilon = f + T\eta$. In practice one would expect ε to be of the order of magnitude of f so that, say, $1 < \varepsilon/f < 10$. The ratio $T_M c / L$ is equal to 14.3 for succinonitrile¹³ and is about 2 for water, so $T_M c / L$ can be believed to be of order 1–10. R can therefore be expected to lie somewhere between 0.1 and 10.

B. The numerical technique

We study Eq. (12) with the help of a method first proposed by Vander-Broeck¹⁴ and then applied to the solidification problem by Meiron⁴ and Kessler and Levine.⁵ The idea is to allow for a possible cusp in $\zeta(x)$ at the tip. A physically acceptable solution must be smooth so the cusp will vanish; this yields a solvability condition. Given d'_0 and R , a solution is numerically computed and then the right slope at the tip λ is examined. When it vanishes we find a steady-state solution with at least a continuous second derivative at $x = 0$.

The integro-differential equation is solved by discretizing the domain of integration and approximating the function by parabolic elements. The resulting system of nonlinear equations is solved by Newton's method. The discretization was changed to check convergence to the

ρ is considered as independent of P and T so that there is no mass transport (we want to ignore convection) and therefore $\alpha = k = 0$. The complete set of equations is then

$$\partial T / \partial t = D \Delta T, \quad (11a)$$

$$T(\text{interface}) = T_M (1 - d_0 \kappa), \quad (11b)$$

$$Dc(\partial T / \partial n|_S - \partial T / \partial n|_L) = Lv_n (1 - d_1 \kappa), \quad (11c)$$

$$T(\text{far from the solid}) = T_\infty < T_M. \quad (11d)$$

Here $d_0 = f/L$, $d_1 = \varepsilon/L$ [by Eq. (9c) with $c_S = c_L$ and $\alpha = k = 0$]. $d_1 > d_0$ since $\varepsilon = f + T\eta$, where η is the surface entropy per unit area.

We transform Eqs. (11) into an integral equation¹²

continuum limit. We used a Control Data Corporation Cyber-205 computer at the John von Neumann Computer Center (Princeton, NJ) (JVNCC). Let us firstly summarize the results that we obtained.

(i) The effect of d_1 on the solvability curve λ versus v is qualitatively different depending on whether $R > 1$ or $R < 1$. For $R > 1$ the curve crosses the abscissa at one point yielding a steady-state solution (Fig. 1). For $R < 1$ the curve is qualitatively similar to the one at $R = 0$ when no anisotropy is present; there are no solutions (the reader can refer ahead to Fig. 3).

(ii) When $R < 1$, the only zeros are produced by the anisotropy (Fig. 3). The zero induced by d_1 when $R > 1$ is stable against the addition of anisotropy (the zero moves towards smaller velocity). In addition, the anisotropy induces new zeros in the λ versus v curve near $v = 0$, just as in the $R < 1$ case. Let us now present and discuss in detail our various results.

1. Steady-state solutions induced by the latent heat term (d_1)

Consider Fig. 1 where we plot the slope at $x = 0$ as a function of d'_0 for $p = 0.10$ and $R = 15$. The slope is zero at $d'_0 = 0.0$ (it corresponds to the Ivantsov solution) and also at $d'_0 = 0.0038$ (remember that $d'_0 = T_M c f v / 2DL^2$, and so d'_0 is proportional to the velocity); there is therefore a nontrivial selected steady state. It was checked with a larger R and a coarser discretization that the curve does not cross the abscissa again for d'_0 large, so we have only one nontrivial steady state.

Let us now check to see if this solution is acceptable, given our model. We know that Eqs. (11b) and (11c) are valid only if $d_0 \kappa \ll 1$ and $d_1 \kappa \ll 1$ everywhere on the interface since higher-order terms in κ were ignored. A solution to the model will be, strictly speaking, acceptable only if it satisfies these two conditions; if the two conditions are not satisfied we cannot justify the truncation to $O(\kappa)$ in Eqs. (11b) and (11c) of the model. A solution that does not satisfy these two conditions is val-

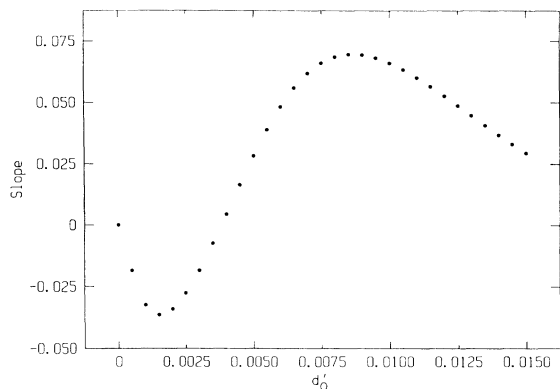


FIG. 1. Slope as a function of d'_0 for $R = d'_1/d'_0 = 15$ and $p = 0.10$. There is no anisotropy.

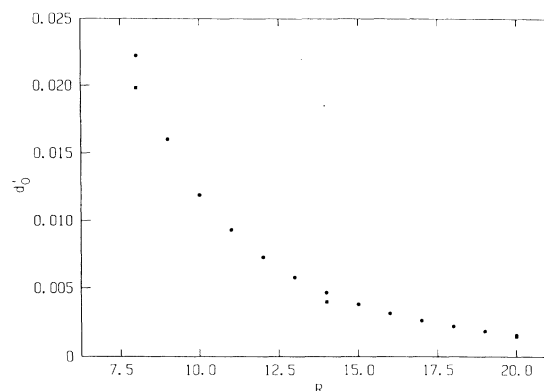


FIG. 2. Selected d'_0 as a function of R . $p = 0.10$ for the dots and $p = 0.12$ for the few squares. There is no anisotropy.

id in the case where Eqs. (11b) and (11c) are valid for arbitrary κ . A solution which is not, strictly speaking, acceptable might nevertheless be qualitatively correct provided that the truncation to $O(\kappa)$ does not dispense with some essential physics.

Let us rewrite the conditions $d_0\kappa \ll 1$ and $d_1\kappa \ll 1$ in terms of the numerical parameters. We checked that the steady-state solutions obtained numerically were very similar to the Ivantsov parabolas with the same velocities; we will use this to approximate the curvature at the tip by ρ^{-1} , where ρ is the Ivantsov radius of curvature satisfying $\rho v/2D = p$. The conditions $d_0\rho^{-1} \ll 1$ and $d_1\rho^{-1} \ll 1$ become $d_0v/2D \ll p$ and $d_1v/2D \ll p$. Using Eq. (13) for the definition of d'_0 and $d'_1 = Rd'_0$, the conditions become

$$d'_0 \ll pT_M c/L, \quad (14)$$

$$d'_0 \ll p/R. \quad (15)$$

Let us now come back to the solution of Fig. 1. Since $T_M c/L$ is typically of order 1–10 we see that the inequality of Eq. (14) is easily satisfied (and this will be true for all the cases considered in this paper). The inequality of Eq. (15) is *not satisfied*, however, since $p/R = 0.0067$, and therefore $d'_0 \approx p/R$. This needle crystal is too sharp to be rigorously described by our model since $\rho \approx d_1$. It is a solution that can thus be, at best, a qualitatively correct manifestation of the exact solution that one would obtain with a model valid for arbitrary large κ . Since the condition $d_0\kappa \ll 1$ is satisfied, the typical scale of the crystal is still much larger than the capillary length.

The properties of these solutions are very counterintuitive. In Fig. 2 we plot the selected value of d'_0 as a function of R ($p = 0.10$ for the dots and $p = 0.12$ for the few squares). We see that the velocity decreases as R increases. If we look back at Fig. 1 this means that the crossing point is shifting towards $d'_0 \rightarrow \infty$ and diverges as d_1 decreases. When $d_1 = 0$ we therefore recover the by now familiar result^{4,5} of a slope everywhere negative. The velocity is also decreasing as the undercooling (i.e., the Péclet number) increases. These results are surpris-

ing since when R increases by increasing the ratio d_1/d_0 while keeping the dimensionless undercooling $T_M c/L$ constant, the latent heat released into the liquid diminishes. Then one would expect the growth velocity to increase; also, when the dimensionless undercooling $\Delta = T_M c/L$ increases the latent heat is evacuated more efficiently in the liquid so once again one would expect that the velocity should increase.

This counterintuitive behavior can, however, be explained. Let us make the hypothesis that the tip region is the region controlling the selection of the velocity since from far away the shape is almost parabolic and there is an Ivantsov solution for any velocity. Approximating again the tip by an Ivantsov parabola we see that by Eq. (11c) the flux of heat near the tip is $q \approx Lv(1 - d_1v/2Dp)$ which has a *maximum* at $v = Dp/d_1$. This last equality can be rewritten as $d'_0 = p/2R$. For $d'_0 > p/2R$ the dendrite must *slow down* to increase the heat flux, so its velocity will decrease if we increase the undercooling. When $d'_0 > p/R$ the heat flux q is even *negative* (near the tip only). This means that heat is flowing towards the solid in the tip region. If R (and therefore d_1) gets larger then the amount of heat flowing towards the solid increases. This has the effect of slowing down the growth. In Fig. 2 we see that $d'_0 > p/R$ ($d_1\kappa > 1$) for small R and $d'_0 \approx p/2R$ ($d_1\kappa \approx 1/2$) for larger R .

The question that we would like to answer is the following: Is it possible to find a range of p and R such that the selected steady state is in the $d_1\kappa \ll 1$ regime? To satisfy Eq. (15) we would like to increase p and hopefully find solutions with small velocities ($d'_0 \ll p/R$). It is, however, not possible to increase p numerically since, as is explained in the Appendix, for large p the slope behaves as $\exp(-2ap/\sqrt{d'_0})$, where a is a number of order unity. For large p we indeed observe numerically that the slope becomes too small for our numerical resolution.

In the Appendix we present an analytical analysis done in the limit $\Delta \rightarrow 1$. It is conjectured that we can find steady-state solutions in the absence of anisotropy provided that $R > 1$. The selected velocity diverges as

$R \rightarrow 1$ (so as $d_1 \rightarrow T_M c d_0 / L$). These solutions do satisfy $d_1 \kappa \ll 1$; however, the selected velocities are still decreasing as the undercooling increases. The explanation of this behavior is unclear. For $R < 1$ there should be no solutions (without anisotropy). All these predictions are consistent with the previous numerical results.

We also studied the effect of anisotropy on these solutions. The addition of anisotropy to both d_0 and d_1 (in the way explained below) has the effect of slightly decreasing the selected velocity.

2. Steady-state solutions induced by anisotropy

In Fig. 3 we plot the slope at $x = 0$ as a function of d'_0 for $p = 1.0$ and $R = 1.0$. The curve with the dots is the result when no anisotropy is included. For the curve with the squares we added some anisotropy to both d_0 and d_1 by multiplying them by $(1 + a \cos\theta \sin\theta)$, where θ is the angle between the growth axis and the normal to the interface. The same anisotropy is added to both terms since they share the same physical origin [$d_0 = f/L$, $d_1 = (f + T\eta)/L$]. a is the anisotropy parameter and is here equal to 0.2. It is clear from these curves that when $R < 1$ anisotropy is needed to obtain a nontrivial steady-state solution; for $a = 0.2$ there is indeed a solution at $d'_0 = 0.022$. Since $p = p/R = 1.0$ clearly the inequalities of Eqs. (14) and (15) are satisfied.

When $R > 1$ we checked (for R up to 10) that the addition of anisotropy was inducing new zeros near $d'_0 \approx 0$ in a way completely similar to Fig. 3. The zero obtained without anisotropy (Fig. 1) was stable and slightly shifted towards a smaller velocity.

In Fig. 4 we show the selected value for d'_0 as a function of R . We see that the velocity increases with R , and thus increases with d_1 , as expected. For the dots, $p = 1.0$ and $a = 0.2$. For the squares, we decrease the undercooling; $p = 0.5$ and $a = 0.2$. As expected, the velocity decreases. For the triangles, we decrease the anisotropy; $p = 1.0$ and $a = 0.1$. The velocity decreases with respect to the dotted curve. In the next figures we

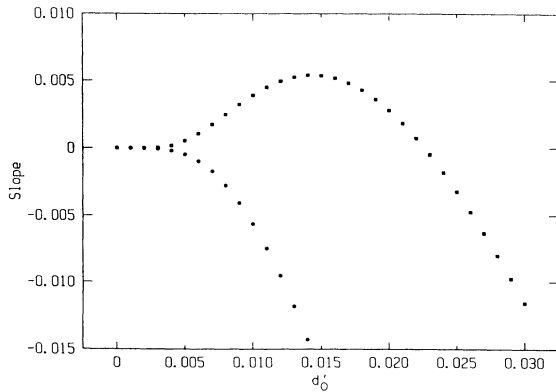


FIG. 3. Slope as a function of d'_0 for $R = 1.0$ and $p = 1.0$. There is no anisotropy for the dots, and $a = 0.2$ for the squares.

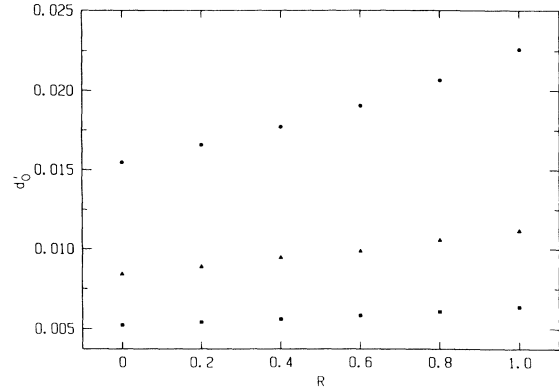


FIG. 4. Selected d'_0 as a function of R . For the dots $p = 1.0$ and $a = 0.2$; for the triangles $p = 1.0$ and $a = 0.1$; for the squares $p = 0.5$ and $a = 0.2$.

study in detail the behavior of the velocity as we vary the anisotropy and the undercooling.

In Fig. 5 we plot the selected d'_0 as a function of the anisotropy (as before anisotropy is added to both d_0 and d_1). Here $p = 0.5$ and $R = 0.4$. The velocity increases with a and saturates to an approximately constant value for $a > 0.6$. This is consistent with what has been observed in a previous work⁶ in the absence of d_1 and in the presence of the kinetic undercooling.

In Fig. 6 the selected d'_0 is plotted as a function of the Péclet number for $R = 1.0$ and $a = 0.2$. As expected, the velocity increases with the undercooling. A log-log plot of this figure is shown in Fig. 7. From this plot we can deduce that the selected d'_0 is proportional to $p^{1.9}$. For $p \rightarrow 0$ we should expect¹⁵ $v \propto \Delta^4$, and so $d_0 a p^2$, and therefore our result (obtained over the range $0.1 < p < 1.0$) is consistent with this prediction. This result implies that as $p \rightarrow 0$ the selected d'_0 will still satisfy $d'_0 \ll p/R$ since $d'_0 a p^2$, so these solutions will satisfy $d_1 \kappa \ll 1$ (and $d_0 \kappa \ll 1$) even in the $\Delta \rightarrow 0$ limit.

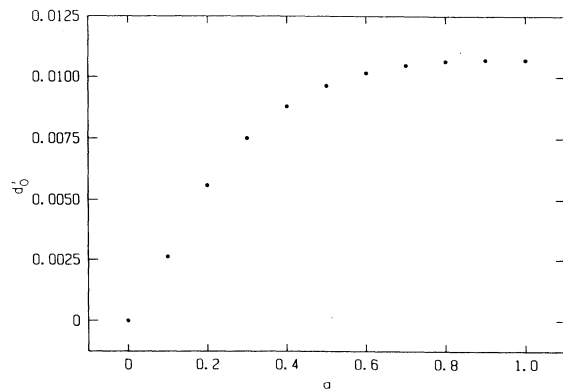


FIG. 5. Selected d'_0 as a function of a , for $p = 0.5$ and $R = 0.4$.

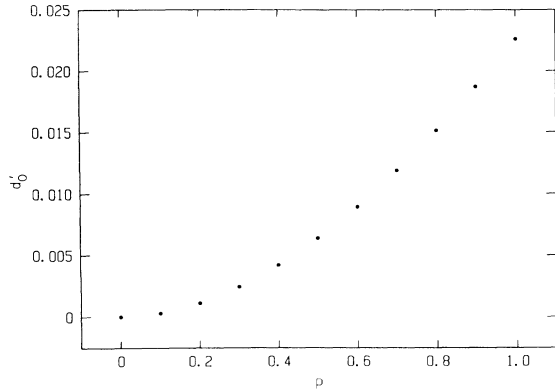


FIG. 6. Selected d'_0 as a function of p , for $R=1.0$ and $a=0.2$.

CONCLUSION

In Sec. I we introduced a curvature correction to the heat-balance equation of the solid-melt interface. This correction should be included in any realistic model of dendritic growth. The correction can be tested by experiments measuring precisely the Mullins-Sekerka dispersion relation.

In Sec. II we showed that this correction, together with the Gibbs-Thomson correction, gives, in the absence of anisotropy, steady-state solutions that do not satisfy $d_1\kappa \ll 1$. These solutions behave counterintuitively since their velocity decreases as d_1 or p increases. They may actually be qualitatively correct if the truncation of Eq. (9a) to order κ does not throw away some essential physics. These solutions could appear in the dynamics as sharp needle crystals that melt back. The addition of anisotropy simply decreases slightly the velocity of these solutions. A plausible analytical conjecture of these solutions is presented in the limit of large undercooling in the Appendix. The analytical solutions do behave counterintuitively but they satisfy the condition $d_1\kappa \ll 1$ so that the reasons explaining their behavior are unclear. It is also predicted in the Appendix that

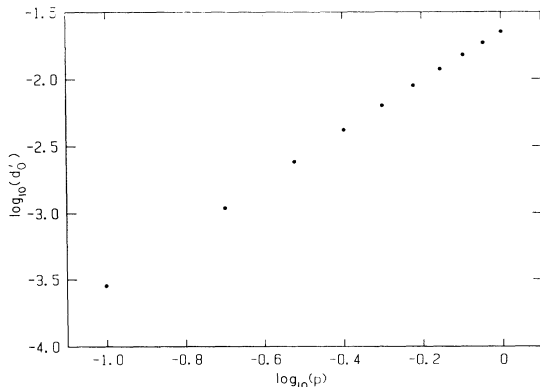


FIG. 7. Log-log plot of Fig. 6.

these solutions exist only when $R > 1$, that is, when $d_1 > T_M c d_0 / L$.

Additional solutions appear for any R when anisotropy is added to d_0 and d_1 . We studied in detail the range $0.1 < R < 1.0$. As expected, the selected velocity increases as d_1 increases. It was found that the velocity saturates to an almost constant value for large anisotropy. We also showed that the velocity was proportional to $p^{1.9} \approx p^2$ in the range $0.1 < p < 1.0$. These solutions were already well known in the limit $d_1=0$.^{4,5,16,17} The addition of d_1 slightly increases the value of the selected velocities.

ACKNOWLEDGMENTS

J. Liu provided the version of the program used for the numerical simulations. He is also thanked for many useful discussions. One of us (M.A.L.) is supported in part by the Natural Sciences and Engineering Research Council (NSERC) of Canada and in part by the Massachusetts Institute of Technology. The other (G.K.) acknowledges support from the Alfred P. Sloan foundation. This work is supported by the National Science Foundation (NSF), Grant No. DMR-84-18718.

APPENDIX: AN ANALYTICAL CONJECTURE IN THE LIMIT OF LARGE UNDERCOOLING

In this appendix we will apply the method developed in Ref. 18 to study the two-dimensional nonlocal model of solidification in the limit of large undercooling and in the presence of d_1 . [It should be pointed out that in the limit of small undercooling ($p \rightarrow 0$ limit) the d_1 term is a higher-order effect in terms of p , the Péclet number]. Our analysis is very similar to the analysis of Ref. 18 and thus our derivation will only be sketched.

We define $\delta \equiv 1 - \Delta$ and we will take the limit $\delta \ll 1$. In this limit the Péclet number becomes $p \approx 1/(2\delta) \gg 1$. The equation of motion of the interface is

$$1 - \delta - d'_0 \kappa [\zeta(x)] = 2 \int_0^\infty d\tau \int_{-\infty}^\infty dx' \{1 - R d'_0 \kappa [\zeta(x')]\} \times G(x, \zeta(x), \tau | x', \zeta(x'), 0), \quad (\text{A1})$$

where

$$G(x, z, \tau | x', z', 0) = (4\pi\tau)^{-1} \exp\{-[(x-x')^2 + (z-z'+2\tau)^2]/4\tau\}. \quad (\text{A2})$$

Here lengths have been expressed in units of $1 = 2D/v$ and time has been expressed in units of $1^2/D$. d'_0 and R are defined as before.

Eq. (A1) can be reduced to a linear, inhomogeneous differential equation of infinite order in the limit $\delta \ll 1$. We first do the change of variables $X = x' - x$ and express $\zeta(x')$ as a Taylor expansion around $\zeta(x)$, the motivation being that in our units $\zeta''(x) \ll 1$. (Here the primes denote derivatives with respect to x .) The Ivantsov parabola is indeed given in our units by

$\zeta''(x) = -2\delta$. The n th derivative of ζ with respect to x can be written as $\zeta^{(n)} \approx (-2\delta d/d\eta)^{n-2} \zeta''$, where $\eta \equiv \zeta'$. It will turn out that the natural variable of the equation will be η , so that we write

$$\zeta'' = -2\delta[1 + h(\eta)] \quad (\text{A3})$$

and we assume that $h \ll 1$. We take the $\delta \ll 1$ limit of Eq. (A1) and we furthermore linearize in terms of h . We get

$$(L_0 - 2\delta L_1 - d'_0 \mu^3) h(\eta) = d'_0(1 - R)\mu^3 + \delta b_0 + O(\delta^2), \quad (\text{A4})$$

where

$$L_0 = \sum_{n=0}^{\infty} a_n(\eta) (-2\delta d/d\eta)^n, \quad (\text{A5})$$

$$L_1 = \sum_{n=0}^{\infty} b_n(\eta) (-2\delta d/d\eta)^n, \quad (\text{A6})$$

$$\mu = (1 + \eta^2)^{-1/2}, \quad (\text{A7})$$

with

$$a_n(\eta) \equiv \int_0^{\infty} d\tau \int_{-\infty}^{\infty} dX g_0(X, \tau | \eta) \{ (2\tau - X\eta) X^{n+2} / [\tau(n+2)!] + 2R d'_0 \mu^3 X^n / n! \}. \quad (\text{A8})$$

$$b_n(\eta) \equiv \int_0^{\infty} d\tau \int_{-\infty}^{\infty} dX g_0(X, \tau | \eta) X^{n+4} [(X\eta - 2\tau)^2 / 2\tau^2 - 1/\tau] / [2(n+2)!] \\ - 2R d'_0 \mu^3 \int_0^{\infty} d\tau \int_{-\infty}^{\infty} dX g_0(X, \tau | \eta) \{ X^{n+2} (X\eta - 2\tau) [1/(n+2)! + \frac{1}{2}(n!)] \\ \times [1/(2\tau)] + 3\mu^2 \eta(n+2) X^{n+1} / [(n+1)!] \} \quad (\text{A9})$$

and

$$g_0(X, \tau | \eta) = (4\pi\tau)^{-1} \exp\{ -[X^2 + (X\eta - 2\tau)^2] / 4\tau \}. \quad (\text{A10})$$

We kept the terms such as $(-2\delta d/d\eta)^n$ to all orders since we will now look for a solution which is essentially singular in δ , more precisely for a solution of the WKB type,

$$h(\eta) = \exp[\delta^{-1} S_0(\eta) + S_1(\eta) + O(\delta)]. \quad (\text{A11})$$

We will first look for homogeneous solutions to (A4). Inserting (A11) into (A4) we get to $O(1)$

$$L_0(S'_0, \eta) = d'_0 \mu^3, \quad (\text{A12})$$

where

$$L_0(S'_0, \eta) = \sum_{n=0}^{\infty} a_n(\eta) (-2S'_0)^n \quad (\text{A13})$$

and $S'_0 \equiv dS_0/d\eta$. To $O(\delta)$ we get

$$S'_1 \partial L_0 / \partial S'_0 + (S''_0 / 2) \partial^2 L_0 / \partial S'^2_0 - 2L_1(S'_0, \eta) = 0, \quad (\text{A14})$$

where

$$L_1(S'_0, \eta) = \sum_{n=0}^{\infty} b_n(\eta) (-2S'_0)^n. \quad (\text{A15})$$

It is possible to perform the sums explicitly in Eqs. (A13) and (A15) and then to carry out the integrals over

$$F(s) = 2\delta^{-1} S'_{0+}(s) S'_{0-}(s) / \{ [S'_{0+}(s) - S'_{0-}(s)] [1 - 2d'_0(1 - R)\mu^3(s)] \}, \quad (\text{A21})$$

When $\eta = \pm\infty$ we are infinitely far from the tip of the growing crystal and therefore the solution must be equal to the Ivantsov solution. This means, by Eq. (A3), that $h_P(\pm\infty) = 0$. This boundary condition was already im-

posed at $\eta = -\infty$ on Eq. (A19). Because both h_+ and h_- diverge as $\eta \rightarrow \pm\infty$ we cannot add any components of h_{\pm} to h_P without disqualifying our solution; we must therefore check if our solution, as it stands, satisfies the

$$\tau \text{ and } X \text{ to get closed-form expressions for } L_0(S'_0, \eta) \text{ and } L_1(S'_0, \eta). \text{ We can in principle solve (A12) for } S'_0 \text{ and then (A14) for } S'_1. \text{ The expressions are, however, quite complicated. They simplify a lot if we look for solutions in the regime } d'_0 \ll 1. \text{ We then get two independent homogeneous solutions,}$$

$$h_{\pm}(\eta) = \exp(\delta^{-1} S_{0\pm} + S_{1\pm} + \dots), \quad (\text{A16})$$

where

$$dS_{0+}/d\eta = i(1 - i\eta)^{3/4} (1 + i\eta)^{1/4} / (2\sqrt{d'_0}) \\ + (\eta - i + iR) / 4 + O(\sqrt{d'_0}), \quad (\text{A17})$$

$$S_{1+} = -3i \arctan(\eta) / 4 \\ + \frac{3}{4} (1 + R) \ln(1 + \eta^2) + O(\sqrt{d'_0}), \quad (\text{A18})$$

and $S_{0,1-}$ is the complex conjugate of $S_{0,1+}$.

We will now try to construct a particular solution to Eq. (A4). Since Eq. (A4) is of infinite order there is no sure way of constructing its particular solution. We make the guess

$$h_P(\eta) = \int_{-\infty}^{\eta} ds \phi(s) F(s) \\ \times [h_+(\eta)/h_+(s) - h_-(\eta)/h_-(s)], \quad (\text{A19})$$

where

$$\phi(s) = d'_0(1 - R)\mu^3(s) + O(\delta). \quad (\text{A20})$$

To determine $F(s)$ we ask for h_P to satisfy Eq. (A4). We obtain to dominant order

boundary condition $h_p(\infty)=0$. This becomes our “solvability condition.” For large η we have

$$h_p(\eta) \approx [h_+(\eta) - h_-(\eta)] I_1(\delta, d'_0, R), \quad \text{as } \eta \rightarrow \infty \quad (\text{A22})$$

with

$$I_1(\delta, d'_0, R) = \int_{-\infty}^{\infty} ds \phi(s) F(s) / h_+(s), \quad (\text{A23})$$

where we used the property $S_{0,1+}(\eta) = S_{0,1-}(-\eta)$. Since h_+ and h_- are independent the condition $h_p(\infty) = 0$ therefore implies

$$I_1(\delta, d'_0, R) = 0. \quad (\text{A24})$$

Using the fact that $\delta \ll 1$ we can evaluate I_1 by using a saddle-point approximation around $\eta = i$. We get

$$I_1(\delta, d'_0, R) \approx N_1 (1-R) (d'_0)^{1/4-3R/14} \times \delta^{-(3/2+3R/7)} \exp[-a/(\delta\sqrt{d'_0})], \quad (\text{A25})$$

where N_1 is some number and $a \approx 0.3079 \dots$. Equation (A24) can be satisfied if $d'_0 = 0$, which corresponds to the Ivantsov solution. For $R \neq 1$ and $\delta \neq 0$ it cannot be satisfied with $d'_0 \neq 0$. It is also apparently satisfied when $R = 1$ and we must investigate the meaning of this peculiar result.

When $R = 1$ the inhomogeneous part of Eq. (A4) is of order δ .

To treat the problem correctly one should therefore do the following.

Write the differential equation (A4) to order δ^2 .

Compute the WKB solution to order δ , i.e., compute $S_2(\eta)$.

Compute $F(s)$ to next order in δ .

Obtain the particular solution to order δ .

One would then obtain a solvability condition conceptually similar to Eq. (A25), but of higher order in δ ,

$$I_2(\delta, d'_0, R=1) = 0. \quad (\text{A26})$$

This solvability condition would not be satisfied for arbitrary δ and d'_0 . Therefore, although Eq. (A24) is satisfied when $R = 1$, we would not get solutions for arbitrary δ and d'_0 .

We can now ask the following question: Is it possible, when $R \neq 1$, to add I_1 to I_2 in such a way that their sum is zero? Let us assume that we can write I_2 to leading order in δ and d'_0 as

$$I_2(\delta, d'_0, R) \approx N_2 (d'_0)^{\alpha(R)} \delta^{\beta(R)} \exp[-a/(\delta\sqrt{d'_0})]. \quad (\text{A27})$$

We expect the same exponential dependence since $\exp(\delta^{-1}S_0)$ will again control the saddle point around $\eta = i$. Adding I_1 to I_2 we get the following solvability condition:

$$(d'_0)^{1/4-3R/14-\alpha(R)} = \delta^{3/2+3R/7+\beta(R)} N_2 / [N_1(R-1)]. \quad (\text{A28})$$

Since I_2 must be a correction of higher order in δ as compared to I_1 we know that $3/2+3R/7+\beta(R) > 0$. We will now make the hypothesis that $1/4-3R/14-\alpha(R) > 0$. This is really a guess, but if it is true, then Eq. (A28) will explain the existence of solutions in the absence of anisotropy. We know that this equation has no solution when $R = 0$ (as was checked numerically^{8,9}). This implies that $N_2/N_1 > 0$ since then the right-hand side is negative which ensures that Eq. (A28) is not solvable (for $R = 0$). With these assumptions we can therefore conclude from Eq. (A28) the following.

(1) For $R < 1$ there are no solutions.

(2) For $R > 1$ the selected velocity behaves like

$$d'_0 \alpha \delta^{[42+12R+28\beta(R)]/[7-6R-28\alpha(R)]} / (R-1). \quad (\text{A29})$$

(3) As $R \rightarrow 1$ the selected velocity diverges. Strictly speaking, for $R \approx 1$ Eq. (A28) is not valid (since it was derived in the limit $d'_0 \ll 1$), but it certainly hints that at least a strong increase in the velocity is to be expected.

All these results are in agreement with the numerical results that are presented in Sec. II of this paper. In particular, the selected d'_0 given by Eq. (A29) decreases as the undercooling increases (thus as δ decreases), and also as d_1 (thus R) increases. It must be noted, however, that Eqs. (14) and (15) of Sec. II are satisfied in this limit and thus that $d_0\kappa \ll 1$ and $d_1\kappa \ll 1$. The explanation of this counterintuitive behavior is, as of now, unknown.

We may finally note that I_1 can be shown to be proportional to $d\kappa/d\theta|_{\theta=0}$. Using the relation $p \approx 1/(2\delta)$ we get

$$d\kappa/d\theta|_{\theta=0} = N'_1 (1-R) (d'_0)^{-1/4-3R/14} \times p^{3/2+3R/7} \exp(-2ap/\sqrt{d'_0}). \quad (\text{A30})$$

The slope at the tip is not related to this quantity in a simple way, but from this equation we can believe that it behaves to leading order like $\exp(-2ap/\sqrt{d'_0})$ which explains the fact that the slope gets too small for our numerical resolution when p is large. This limited the scope of our numerical study.

¹E. Ben-Jacob, N. Goldenfeld, B. G. Kotliar, and J. S. Langer, Phys. Rev. Lett. **53**, 2110 (1984).

²D. Kessler, J. Koplik, and H. Levine, Phys. Rev. A **31**, 1712 (1985).

³D. Kessler, J. Koplik, and H. Levine (unpublished).

⁴D. I. Meiron, Phys. Rev. A **33**, 2704 (1986).

⁵D. A. Kessler and H. Levine, Phys. Rev. B **33**, 7867 (1986).

⁶M.-A. Lemieux, J. Liu, and G. Kotliar, Phys. Rev. A **36**, 1849 (1987).

⁷J. W. Cahn, Acta Metall. **28**, 1333 (1980).

⁸J. W. Gibbs, *Collected Works* (Yale University Press, New Haven, 1957), Vol. 1, pp. 314–331.

- ⁹Ref. 8, footnote of p. 315.
- ¹⁰W. W. Mullins and R. F. Sekerka, *J. Appl. Phys.* **35**, 444 (1964).
- ¹¹J. S. Langer, *Rev. Mod. Phys.* **52**, 1 (1980).
- ¹²G. C. Nash and M. E. Glicksman, *Acta Metall.* **22**, 1283 (1974).
- ¹³M. E. Glicksman, R. J. Schaefer, and J. D. Ayers, *Metall. Trans.* **7A**, 1747 (1976).
- ¹⁴J.-M. Vander-Broeck, *Phys. Fluids* **26**, 2033 (1983).
- ¹⁵P. Pelce and Y. Pomeau, *Stud. Appl. Math.* **74**, 245 (1986).
- ¹⁶A. Barbieri, D. C. Hong, and J. C. Langer, *Phys. Rev. A* **35**, 1802 (1987).
- ¹⁷D. A. Kessler, J. Koplik, and H. Levine, *Phys. Rev. A* **34**, 4980 (1986).
- ¹⁸B. Caroli, C. Caroli, B. Roulet, and J. S. Langer, *Phys. Rev. A* **33**, 442 (1986).